# Effects of Liquid Metal Walls on Equilibrium and Stability in Tokamaks

A. Y. Aydemir
*Institute for Fusion Studies*
*The University of Texas at Austin*
*Austin, TX 78712 USA*

## Abstract

Liquid metal wall concept has received a great deal of attention recently because of its perceived advantages in addressing high heat flux, magnetohydrodynamic (MHD) stability, and other related issues in advanced confinement schemes. Despite its inherent and clear benefits, this concept also poses potentially serious problems from the MHD equilibrium and stability point of view. In particular, a liquid metal flow strong enough to stabilize resistive wall modes can also have adverse affects on the MHD equilibrium through its interaction with the background poloidal and toroidal fields. These deleterious effects can be large enough to mitigate any expected stabilization of the unstable MHD modes.

## I. INTRODUCTION

Liquid metal wall concept in magnetic fusion is not new. It has already been proposed and studied both as a potential blanket and first wall[1–3]. Perhaps its recent revival[4–6] is due to a realization in the fusion community that the next generation of experiments based on various advanced-concept designs will require handling of much higher heat loads on the first wall, and because of much higher plasma $\beta$'s (plasma pressure normalized to the equilibrium magnetic pressure), they will have much more stringent MHD stability requirements. A flowing liquid metal wall, usually assumed to be molten lithium, would help alleviate both those concerns: it can carry away the generated heat to an external point where it can be recovered. And since it is a conductor, it can also help with MHD stability by providing a very close fitting conducting surface that is continuously in motion relative to the plasma. It is well known that a stationary resistive wall cannot change the MHD stability boundaries[7]. A wall that is in relative motion with respect to the plasma column, however, can stabilize the surviving resistive wall modes (RWM's), simply by screening out the perturbed fields and preventing them from locking to the wall.

Although heat load concerns are obviously important, our discussion of the liquid metal walls will be entirely in the context of MHD equilibrium and stability. The stability discussion will be limited to a general examination of the approximate requirements on the wall flow velocity. We will, however, examine in considerable detail the effects of the liquid metal flow on the equilibrium fields, starting with the premise that the flow is strong enough to stabilize resistive wall modes.

This is essentially a computational study. The three dimensional MHD code **CTD** used in the study will be introduced in the next section. Section III will briefly introduce the resistive wall modes and a simple argument for their stabilization by a flowing liquid metal wall. Section IV will look at the effects of this flow on the background equilibrium fields and point out some potentially serious problems. Section V will present a summary of the results.

## II. THE COMPUTATIONAL MODEL

Our three dimensional, toroidal, nonlinear MHD code, **CTD**[8,9], has been modified to include a vacuum region and a resistive wall in order to study the stability and nonlinear evolution of external kink modes. The recent extension of the resistive wall to allow for arbitrary "fluid motions" makes it possible for us to examine the role of liquid metal walls in controlling these MHD modes. The equations solved by **CTD**, written in nondimensional form, are

$$\frac{\partial \rho}{\partial t} + \nabla \cdot (\rho \mathbf{u}) = \mathbf{0} \tag{1}$$

$$\rho \left\{ \frac{\partial \mathbf{u}}{\partial t} + \mathbf{u} \cdot \nabla \mathbf{u} \right\} = \mathbf{J} \times \mathbf{B} - \nabla p + \mu_i \nabla^2 \mathbf{u}, \tag{2}$$

$$\frac{\partial \mathbf{A}}{\partial t} = \mathbf{u} \times \mathbf{B} - \eta \mathbf{J} - \nabla \times \mu \nabla \times \mathbf{J}, \tag{3}$$

$$\frac{\partial p}{\partial t} + \mathbf{u} \cdot \nabla p = -\Gamma p \nabla \cdot \mathbf{u} + \kappa_{\|} \nabla_{\|}^2 p + \nabla \cdot (\kappa_{\perp} \nabla p) + (\Gamma - 1) \eta J^2. \tag{4}$$

The resistivity is a three dimensional function of temperature and possibly other fields: $\eta = \eta(p(\mathbf{r}, t), \mathbf{r}, t)$. The coefficients $\kappa_{\|}$ and $\kappa_{\perp}$ are the parallel and perpendicular thermal conductivities, respectively, and $\Gamma$ is the ratio of specific heats. The electron viscosity (hyper-resistivity) term in the Ohm's law, which was used in a previous study examining fast sawtooth crashes[10], will not be used in this work ($\mu = 0$).

Noncircular geometries are treated using a conformal transform[11,12,10] from the configuration space to a unit circle in the computational domain. This technique has proven to be highly efficient compared to alternatives when the boundary deformation is not too severe.

The MHD equilibria used here are calculated self-consistently with **CTD** in the presence of various transport processes, and external currents that provide shaping and toroidal equilibrium. Although the code is fully three dimensional, because of the nature of the problem, this study will assume axisymmetry and will be only in two dimensions.

The next section briefly introduces the resistive wall modes and their stabilization by rotation.

## III. RESISTIVE WALL MODES AND ROTATIONAL STABILIZATION

According to a well-known theorem of MHD stability theory[7], stability boundaries cannot be changed by introducing a resistive wall near the plasma. Thus, an external mode stabilized by a close-fitting "perfect" conductor will in fact grow on the slow $L/R$ time of the (resistive) wall. In our nondimensional units, for a wall of thickness $\delta$, minor radius $a$, and resistivity $\eta$, the resistive wall time is $\tau_W = a\delta/\eta$. Defining a characteristic wall frequency as $\Omega_W = 2\pi/\tau_W$, we can look at the resistive wall as a "low-pass filter" that screens out waves with frequencies much higher than $\Omega_W$. Unfortunately, an external mode can still lock to the wall and grow at the rate $\gamma \sim 1/\tau_W$, which is precisely what a resistive wall mode does.

If we introduce a relative motion between the mode and the wall by rotating the wall with some velocity $\mathbf{u}$, for example, then a mode in the laboratory frame with frequency and wavenumber $(\omega, \mathbf{k})$ will have a Doppler shifted "rotation frequency" $\Omega_R = \omega + \mathbf{k} \cdot \mathbf{u}$ in the rest frame of the wall. Then it is easy to see that for $\Omega_R \geq \Omega_W$, the perturbed fields due to the mode will be screened out - the wall will act as a "perfect" conductor - and the mode will tend to be stabilized.

This simple argument of course leaves out many of the complications of a real plasma-wall system, but it nevertheless provides the basis for all "rotational stabilization" schemes for the resistive wall modes. More detailed theories predict stabilization of RWM's for wall velocities of the order of $20m/sec.$[13,14] for liquid lithium. For a wall of thickness $\delta = 1cm$, minor radius $a = 1m$, and conductivity $\mu_0\sigma = 4sec/m^2$, this velocity corresponds to a normalized rotation frequency of $\Omega_R/\Omega_W = 0.13$. Note that $\Omega_R/\Omega_W = u\delta/2\pi\eta$ for $k = 1/a$. Thus, our normalized rotation frequency is related to the wall magnetic Reynolds number by $S_W = 2\pi\Omega_R/\Omega_W$ (In SI units, $S_W = \mu_0\sigma u\delta$.). We see that stabilization requires, perhaps not surprisingly, $S_W \sim O(1)$. In the remainder of this paper, $\Omega_R/\Omega_W = 0.1$ will be used as a typical wall rotation frequency. Note that although this frequency was chosen on the basis of resistive stability arguments, it is also comparable to the values one arrives at by other considerations such as the requirements for the heat transfer rate[2].

The next section looks at the effects of rotation on the equilibrium fields.

## IV. EFFECTS OF ROTATING LIQUID METAL WALLS ON THE EQUILIBRIUM FIELDS

In the previous section, we saw that $\Omega_R/\Omega_W \sim 0.1$ is necessary to stabilize the resistive wall modes. Unfortunately, a rotating wall will also affect the equilibrium fields in rather obvious ways. If $|\mathbf{k}_{eq} \cdot \mathbf{u}| \geq \Omega_W$, where the wave vector $\mathbf{k}_{eq}$ now characterizes the spatial variation of these fields, they will be either "frozen-in" the liquid metal and get dragged by it, if they have already penetrated the fluid, or they will be shielded, like the perturbed fields of an unstable mode. Both scenarios will generate large volume and surface currents in the liquid metal, as we will see later in this section.

Note that there is a well-known equilibrium flow that does not disturb the background fields[15]. This flow has the form

$$\mathbf{u}_{eq} = \frac{F(\psi)}{\rho}\mathbf{B} + R^2\Omega(\psi)\nabla\zeta, \tag{5}$$

where $F(\psi)$, and $\Omega(\psi)$ are arbitrary flux functions, $\rho$ is the mass density, and $\zeta$ is the toroidal angle. It is easily seen that $\mathbf{u}_{eq}$ can be purely toroidal but cannot be purely poloidal. Thus, poloidal liquid metal flows will inevitably modify the equilibrium fields.

In the following subsections, we will examine the consequences of violating this equilibrium condition. The flows we consider in this work will not be self-consistent: a flow velocity field will be imposed on the "liquid metal" boundary of our computational domain. Although its effects on the magnetic fields will be calculated consistently and accurately, the back reaction of the currents generated in the liquid metal on the flow itself will be ignored. A fully self-consistent treatment of the problem is left for a future publication.

Below, we first will look at the effects of a nonconforming flow that intersects poloidal fields lines.

### A. Interaction of the flow with the equilibrium poloidal field

Although it is generally assumed that the liquid metal flow would conform to the flux surfaces, for a flow of finite thickness this arrangement is difficult, if not impossible, to ensure. Thus, it is sensible to investigate the consequences of a flow that intersects poloidal field lines. As stated earlier, here we will be concerned only with the effects of the flow on

the equilibrium fields; the related but logically separate problem of having the flow strongly impeded in this nonconforming geometry will be ignored.

The deleterious effects of the flow are graphically demonstrated in Fig. 1, which shows the pressure contours co-rotating with the flow in an elongated, n=0 unstable, equilibrium. Here the wall rotation frequency is $\Omega_R = 1.0 \times 10^{-2}$ (for $k = 1/a$). The parameters for the liquid metal are such that $\Omega_R/\Omega_W = 1.0$ (This larger value was used here in seeking stability for the $n = 0$ mode.). The plasma rotates somewhat more slowly than the wall, with a frequency $\Omega_{plasma} = 7.6 \times 10^{-3}$. The rotation frequency of the plasma obviously depends on various dissipative effects in the plasma, a topic that will not be investigated here. Figure 2 shows location of the magnetic axis as a function of time for two different rotation frequencies. Figure 2(a) corresponds to Fig. 1 and has $\Omega_R/\Omega_W = 1.0$; in Fig. 2(b) the rotation is slower, with $\Omega_R/\Omega_W = 0.1$.

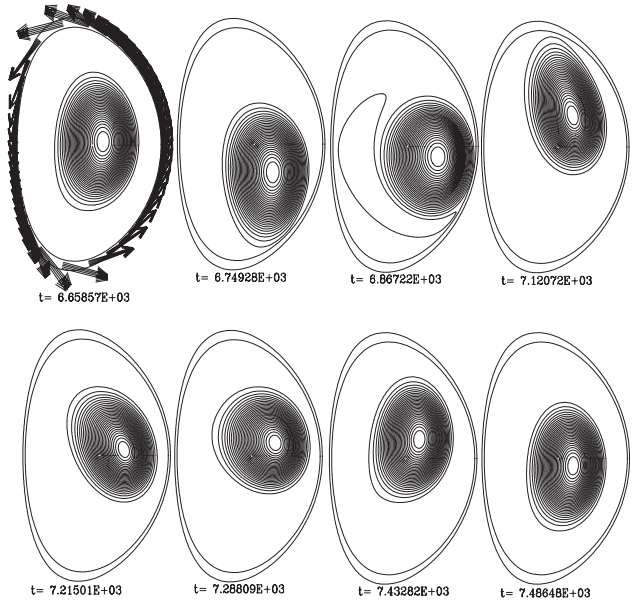


FIG. 1: Pressure contours showing the effects of a uniformly rotating liquid metal wall, as represented by the thin layer on the outside between two boundary lines, in an elongated, $n = 0$ unstable equilibrium. Here $\Omega_R/\Omega_W = 1.0$. The velocity vectors are shown only in the first frame to conserve space.

Although it is not obvious in Fig. 2(b), where the calculation has not been carried out for long enough times, Fig. 2(a) clearly shows the growing amplitude of the oscillations. The plasma column makes larger excursions both in vertical and radial directions with each period of the rotation. Whether this growth in the amplitude is a remnant of the original vertical instability that has not been quite stabilized even with these fast wall rotations, or

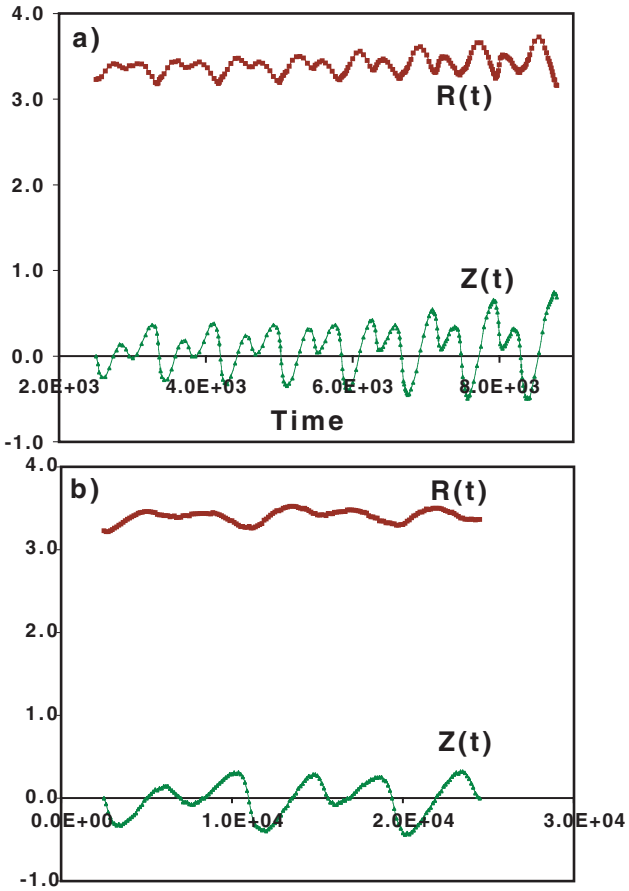


FIG. 2: Location of the magnetic axis as a function of time for uniform wall rotation. a) $\Omega_R/\Omega_W = 1.0$, b) $\Omega_R/\Omega_W = 0.1$

if it is due to some slow change in the equilibrium itself, is not clear at this point. But what is clear is that a poloidally rotating liquid metal wall in this geometry does not appear to be a viable option because of its large-scale effects on the equilibrium.

We have also considered a vertical flow pattern (Fig. 3) that was suggested by Woolley[4]. The initial equilibrium is the same as in Fig. 1. Again, this rather fast flow ($\Omega_R/\Omega_W = 1$) leads to a complex dynamical behavior that does not seem to approach a steady-state (Fig. 4), although the $(R, Z)$ excursions are smaller here than in the uniform rotation case above. The time-span covered by the plot is over 50 transit times ($\tau_{trans} \equiv \pi a/u_{max} = \pi/\Omega_R$).

Note that both for the uniform and vertical flows, the effects on the equilibrium dominate over, and in fact replace, any expected stabilization of the vertical instability by the flows.

In this section, we looked at the interaction of the liquid metal flow with the equilibrium

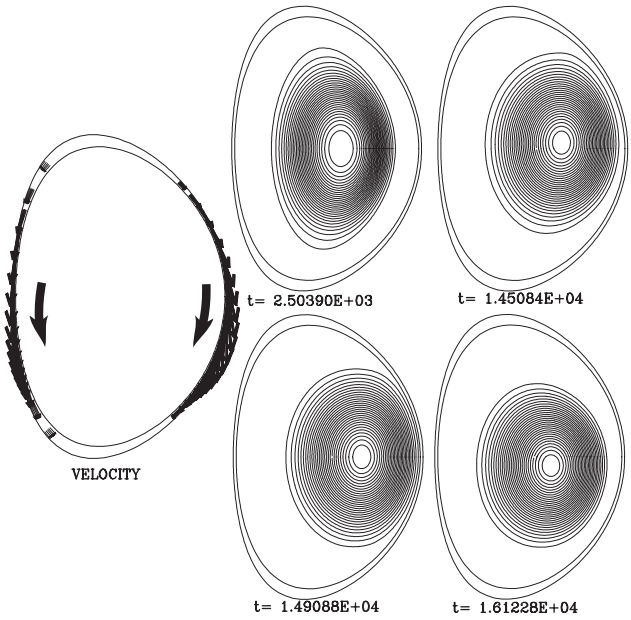


FIG. 3: The velocity vectors for a vertical liquid metal flow and its effect on the equilibrium, as shown by the evolution of the pressure contours. Again $\Omega_R/\Omega_W = 1.0$, where the rotation frequency $\Omega_R \equiv u_{max}/a$.

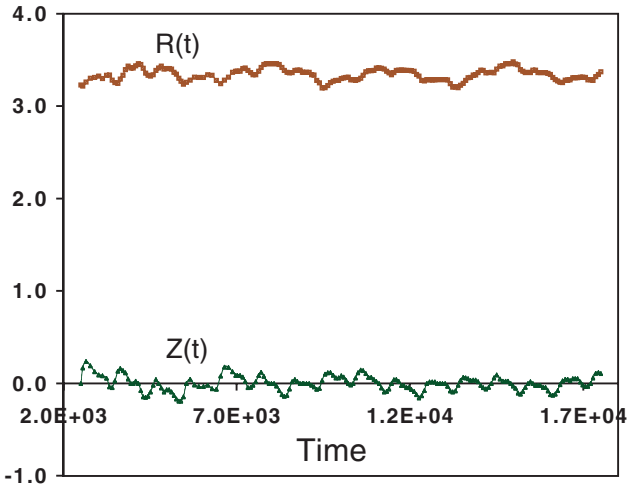


FIG. 4: Location of the magnetic axis as a function of time with a vertically flowing liquid metal wall.

poloidal field. Next, we look at the effects of the equilibrium toroidal field.

### B. Interaction of the flow with the equilibrium toroidal field

Even if the liquid metal flow can be made to conform to the poloidal flux surfaces exactly, its interaction with the generally much larger toroidal field is unavoidable (unless the flow is

purely toroidal). In order to minimize the problems associated with poloidal fields, here we simplify the geometry and examine the problem in an equilibrium with circular cross-section. Some of the relevant equilibrium fields are shown in Fig. 5.

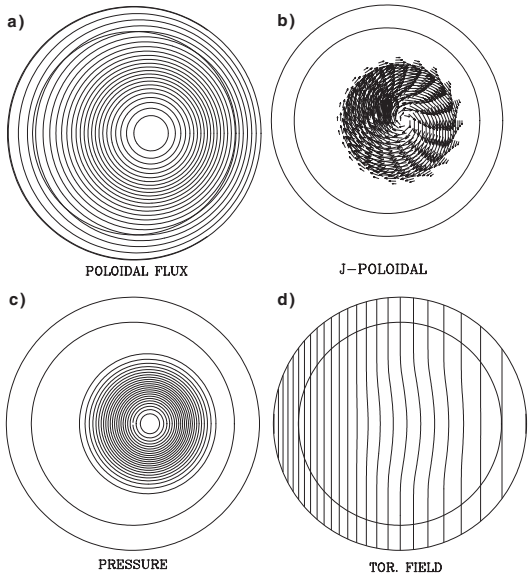


FIG. 5: Various fields for the circular cross-section equilibrium. a) Poloidal flux, b) Equilibrium poloidal currents in the plasma, c) Pressure, d) Contours of toroidal field. The equilibrium toroidal field is in the $-\zeta$ direction (into the plane of the paper) in our $(r, \theta, \zeta)$ coordinate system.

In order to clearly illustrate the generated poloidal currents, the flow layer-width in some of the calculations presented here will have a rather large value of $\delta = 0.25$ in our nondimensional units (in the same units, the minor radius $a = 1.2$ and the major radius $R_0 = 3$ for the circular geometry calculations). The results and the conclusions are not affected if the normalized rotation frequency, $\Omega_R/\Omega_W$, is held constant as the layer width is reduced. In fact, results from the end of this section will use $\delta = 0.05$, as in the previous section on poloidal fields.

The first set of calculations in this geometry, shown in Fig. 6, again has a uniformly rotating wall with $u_\theta = r\Omega_R$. In this section, unless otherwise stated, we will use $\Omega_R/\Omega_W = 0.1$, which corresponds to a wall magnetic Reynolds number of $S_W = 2\pi\Omega_R/\Omega_W = 0.63$. The two most significant results of these calculations are the large magnitude and the undesirable direction of the poloidal currents generated in the wall, as seen in Fig. 6(b): the poloidal current density in the wall is larger than the equilibrium poloidal current density in the plasma. In fact, $J_\theta^{max} \simeq 0.78$, which is approximately 40% of the equilibrium toroidal cur-

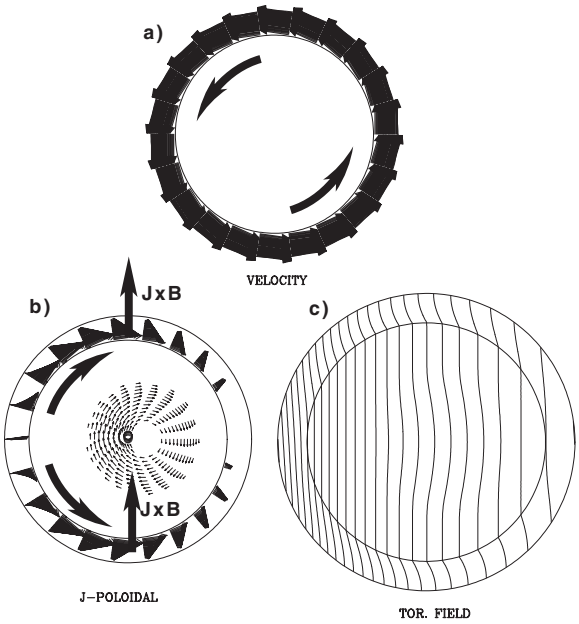


FIG. 6: Rigid rotation with $\Omega_R/\Omega_W = 0.1$. a) Velocity field in the wall. b) Poloidal current density vectors in the wall and plasma. Note that on the scale of the wall currents, the poloidal plasma currents seem negligibly small. c) Toroidal field, showing modification of the field in the wall due to the rotation.

rent density in the center of the plasma column. (In our nondimensional units, $J_{\zeta 0} \simeq 2$ for $q_0 \simeq 1$.) In addition, in the lower half of the chamber the currents are in the $+\theta$ direction, giving rise to a $\mathbf{J} \times \mathbf{B}$ force that will tend to detach the liquid metal from the outer wall and push it into the plasma.

Naively reversing the flow direction in half of the chamber, instead of solving the detachment problem, only exacerbates it, as seen in Fig. 7. Here the liquid metal flow velocity has a $-\sin\theta$ variation that we use to approximate a flow from the inboard to the outboard midplane both in the upper and lower halves of the chamber. This change in the poloidal velocity of the liquid has two important consequences: i) The poloidal current profile in the wall rotates 90° (compared to Fig. 6) while essentially maintaining its overall structure. Again, in half of the chamber the resulting $\mathbf{J} \times \mathbf{B}$ forces are in the "wrong" direction - they will tend to detach the flow from the supporting wall. ii) The maximum current density is now $J_\theta^{max} \simeq 2.2$, approximately three times larger than in the uniform rotation case. We will show in a simple analysis below that, for this flow pattern, the maximum is expected to be larger by a factor of the aspect ratio. Note that $J_\theta^{max}$ here is in fact larger than the toroidal

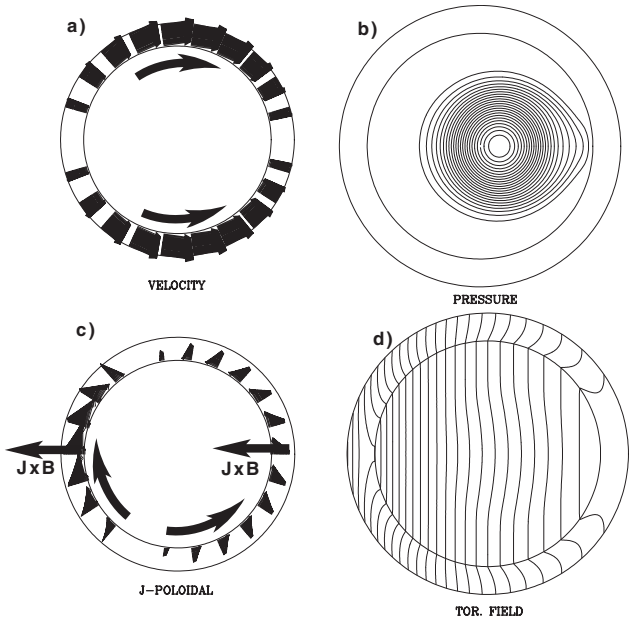


FIG. 7: Liquid metal flow with a $\sin\theta$ variation. a) Velocity field in the wall. b) Pressure contours. Note the "ballooning" on the outboard side. c) Poloidal current density vectors in the wall. The plasma currents are not visible on this scale. Note the direction of the $\mathbf{J} \times \mathbf{B}$ forces. d) Contours of $B_{tor}$.

current density at the magnetic axis of the plasma column! (Recall that wall Reynolds number $S_W = 2\pi\Omega_R/\Omega_W = 0.63$ still.) An additional disturbing effect is the ballooning of the pressure contours seen in Fig. 7(b), which gets worse for higher flow velocities. We have not studied this anomaly in detail, but it appears to be caused by the diamagnetic currents in the low-field side of the chamber that weaken the toroidal field between the plasma column and the boundary.

A final variation on the flow profile is shown in Fig. 8, where the liquid metal flows vertically down along the sides of the chamber, with a $-\cos\theta$ poloidal variation[4].

Here the wall thickness has the more usual value of $\delta = 0.05$, and the velocity amplitude has been adjusted to maintain $\Omega_R/\Omega_W = 0.1$. Surprisingly, this flow geometry produces poloidal currents (Fig. 8(b)) very similar to those in the uniform rotation case of Fig. 6, although $J_\theta^{max}$ here is again higher by about a factor of three. Note that the lower portions of the flow would tend to detach from the supporting wall.

The results of this section can be summarized as follows: All three liquid metal flow geometries, that is, the uniform rotation, and the flows with $\sin\theta$, or $\cos\theta$ variation, produce significant poloidal currents in the liquid metal. This result does not seem to have been anticipated by earlier studies[4–6]. The maximum amplitude for the current density is larger

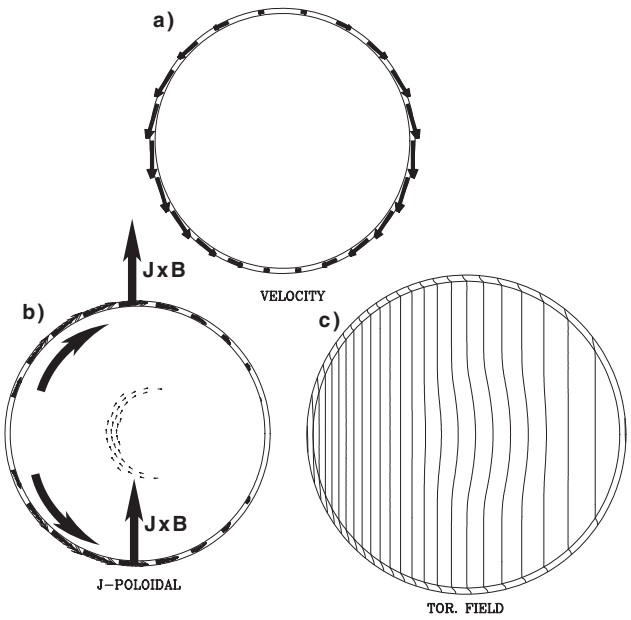


FIG. 8: Liquid metal flow with a $\cos\theta$ variation. a) Velocity field in the wall. b) Poloidal current density vectors in the wall and plasma. Note the direction of the $\mathbf{J}\times\mathbf{B}$ forces. c) Contours of $B_{tor}$.

by a factor of the aspect ratio for the nonuniform cases, a point that will be discussed further in the next section. For the wall Reynolds number of $S_W = 0.63$ used in these calculations, the maximum current density is comparable to the plasma current density at the magnetic axis for typical safety-factor profiles. Finally, in none of the cases is the current poloidally uniform but exhibits a $\sin\theta$, or $\cos\theta$ variation. Thus, the resulting $\mathbf{J}\times\mathbf{B}$ forces point radially inward into the plasma in approximately half of the chamber, which will detach the flow from the supporting wall.

In the next section, we present a simple analysis of these results.

### C. Analysis of the circular-geometry results

Here we present an analysis of the poloidal currents in the liquid metal layer that is in very good agreement with the numerical results of the previous section. The geometry we consider, shown in Fig. 9, is a circular torus of minor radius $a$, major radius $R_0$, and a circular liquid metal layer of thickness $\delta$.

In steady-state, the electric field in the liquid metal will be of the form

$$\mathbf{E} = -\mathbf{u}\times\mathbf{B} + \eta\mathbf{J} = -\nabla\phi. \tag{6}$$

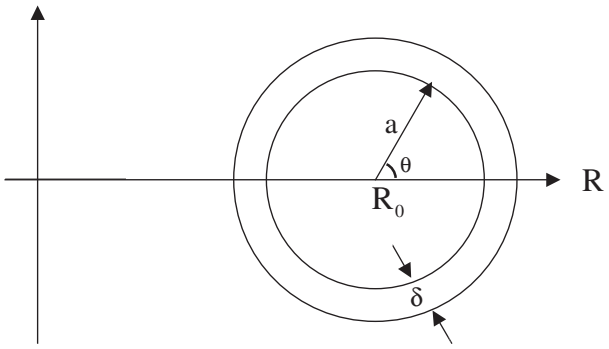


FIG. 9: The geometry used in the analysis of the poloidal currents in the liquid metal wall. The coordinate system is $(r, \theta, \zeta)$, with the $\zeta$ direction out of the plane of the paper.

We ignore toroidal flows and set $u_\zeta = 0$. From the incompressibility of the liquid flow, we have $u_r/u_\theta \sim O(\delta/a)$; thus, with $\delta/a \ll 1$, we can also ignore the radial component of the velocity. Then the poloidal component is assumed to have the form

$$u_\theta(r, \theta) = r\Omega_R f(\theta), \tag{7}$$

where $f(\theta)$ is some function to be specified.

Writing the toroidal field as $B_\zeta = B_{\zeta 0}/\{1 + (r/R_0)\cos\theta\}$ and integrating the radial component of Eq. (6) with the boundary condition $\phi(a + \delta, \theta) = 0$, we obtain for the potential on the inner surface of the liquid metal layer:

$$\phi(r = a, \theta) = -\delta a \Omega_R B_{\zeta 0} f(\theta)(1 - \epsilon\cos\theta + \epsilon^2\cos^2\theta), \tag{8}$$

where we ignored terms of order $(\delta/a)^2$ but retained up to second-order terms in the inverse aspect ratio $\epsilon = a/R_0$. Then using $J_\theta \simeq E_\theta/\eta$, we have the following poloidal current density profiles for the three cases presented in the previous section:

$$J_\theta(a, \theta) = \begin{cases} \epsilon S_W \frac{B_{\zeta 0}}{a}(\sin\theta - \epsilon\sin 2\theta), \;\; f(\theta) = 1, \\ -S_W \frac{B_{\zeta 0}}{a}(\cos\theta - \epsilon\cos 2\theta), \;\; f(\theta) = -\sin\theta, \\ S_W \frac{B_{\zeta 0}}{a}(\sin\theta - \epsilon\sin 2\theta), \;\; f(\theta) = -\cos\theta, \end{cases} \tag{9}$$

where we recall $S_W = 2\pi\Omega_R/\Omega_W$ is the Reynolds number for the wall (In SI units, $S_W = \mu_0\sigma u_\theta \delta$.) The physical mechanism giving rise to these currents is simple: interaction of the poloidal flow with the toroidal field generates a potential difference between

the outer supporting wall and the inner surface of the liquid metal. The poloidal variation of this potential is the source of the currents given in Eq. 9.

Note that the current density increases linearly with the wall magnetic Reynolds number $S_W$. As already stated in the previous section, the currents are smaller by a factor of $\epsilon$ for the uniform rotation case ($f = 1$), and surprisingly, the uniform rotation and vertical flows ($f = -\cos\theta$) both have the same poloidal current distributions. The maximum current density and its poloidal location for each of these cases are given below (using $\epsilon = a/R_0 = 1.2/3 = 0.4$):

$$J_\theta^{max} = \begin{cases} 0.486\ S_W \frac{B_{\zeta 0}}{a} \text{ at } \theta = \pm 0.205,\ f = 1, \\ 1.40\ \ S_W \frac{B_{\zeta 0}}{a} \text{ at } \theta = \pi,\ f = -\sin\theta, \\ 1.215\ S_W \frac{B_{\zeta 0}}{a} \text{ at } \theta = \pm 0.205,\ f = -\cos\theta. \end{cases} \tag{10}$$

A comparison of these results with the numerical calculations of the previous section is shown in Fig. 10. The maximum poloidal current density in the wall is plotted as a function of the normalized frequency $\Omega_R/\Omega_W = S_W/2\pi$ for $f = 1$ and $f = -\sin\theta$. The agreement is excellent for rotation frequencies of up to $\Omega_R/\Omega_W \sim 1$.

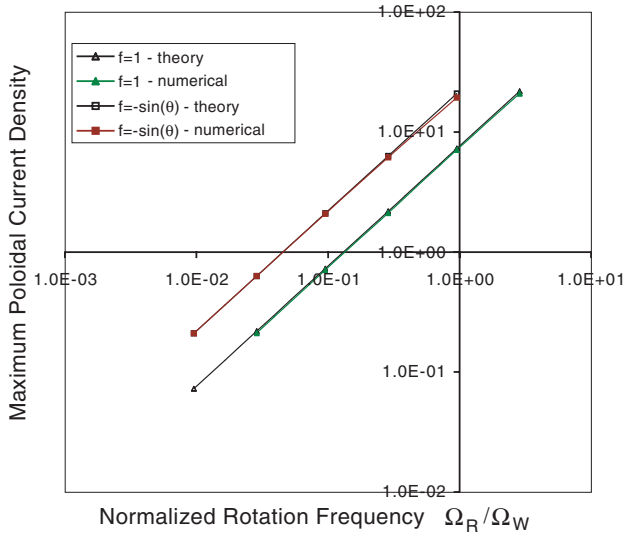


FIG. 10: Maximum poloidal current density in the wall as a function of the normalized rotation frequency. Numerical results are compared with the analysis of this section for two different cases: $f(\theta) = 1$, and $f(\theta) = -\sin\theta$.

It is instructive to give some numerical values for the maximum current density expected

in the liquid metal based on Eq. 10. Assuming a wall Reynolds number of $S_W = 1$ (necessary to stabilize the resistive wall modes[13,14]), and using $a = 1.2m$, $R_0 = 3m$, $B_{\zeta 0} = 5T$, for the $f = -\cos\theta$ case (vertical flow) we get $J_\theta^{max} = 4.06 \times 10^6\ A/m^2$. This value is approximately $4 \times 10^3$ times larger (for the same field strength) than the current density necessary to compensate for the gravitational forces as calculated by Woolley[4]. Note that the corresponding current density for the $f = -\sin\theta$ case would be about $4.68 \times 10^6 A/m^2$.

## V. DISCUSSION AND SUMMARY

Clearly there are significant advantages to having a liquid metal first wall. It can effectively deal with high heat loads, and it can stabilize resistive wall modes, remnants of the external modes that survive with a conventional resistive wall. However, the explicit goal of this work was not to further expound on the virtues of this concept but to point out some of the potential problems. Starting with the assumption, now supported by a number of studies[13,14], that the complete stabilization of external modes requires $S_W = 2\pi\Omega_R/\Omega_W \sim 1$, we have examined the effects of a liquid metal flow of this magnitude on the magnetohydrodynamic equilibrium, and to some degree, stability, of a number of configurations.

When the liquid metal flow does not conform to flux surfaces, as in our studies of elongated equilibria unstable to the vertical $n = 0$ mode, we find that the interaction of the flow with the poloidal field modifies the equilibrium to such an extent that any stabilizing effect becomes irrelevant. A uniformly rotating flow rotates with it the plasma column itself. A nonuniform vertical flow that avoids the X-points of our double-null equilibria also leads to large-amplitude and persistent (R,Z) excursions of the magnetic axis. With such large scale effects on the original equilibria, both these options are probably not viable. It is possible that these negative effects of the flow can be minimized by ensuring that flow conforms to flux surfaces. With a very thin layer of liquid metal, it may be possible to approximately satisfy this condition; it is probably not feasible with a thick layer envisioned in some scenarios.

Even if the flow were perfectly conforming, the effects of the toroidal field would still need to be considered. In three different flow geometries, we showed that the interaction of the moving conducting liquid with the large toroidal field induces large poloidal currents in the liquid metal wall. For velocities such that $S_W \sim 1$, the maximum current density in the liquid metal exceeds the plasma current density at the magnetic axis for typical tokamak

equilibria with $q_0 \simeq 1$. Again, this is a surprising result that does not seem to have been anticipated or fully appreciated in recent studies[4–6,14]. In addition to their large amplitude, the direction of these currents also pose a serious problem. With all three flow patterns, the currents flow in opposite directions in two opposing halves of the chamber; thus, the resulting $\mathbf{J} \times \mathbf{B}$ forces push the liquid against the supporting wall in one half of the chamber and into the plasma in the other half, which would detach the flow from the wall. The current densities expected here are more than three orders of magnitude larger than those assumed by earlier studies[4].

The problems discussed here may not be insurmountable. A flow with a $\sin\theta$ poloidal variation driven by an externally induced and continuous poloidal current potentially solves the detachment problem[14] by ensuring that forces are radially outward everywhere. However, in order to overcome the flow-driven currents, this externally driven current has to be larger than $\sim 1MA$ for the parameters that we have been using. Also, the combination of externally-driven and flow-driven currents will lead to a highly nonuniform poloidal current density distribution, and the effects of this nonuniformity on the flow and the equilibrium would have to be examined carefully.

In the future, we plan to improve and extend this work in a number of directions. Here we entirely ignored the effects of the currents and fields on the liquid metal flow itself, since the flow velocity was prescribed externally. The flow needs to be made self-consistent by allowing the fields to modify it. Only then will we be able to study such topics as the MHD stability of the liquid metal layer, and the magnetic drive mechanism proposed by Zakharov[14]. Also, even in circular geometry we saw that the plasma equilibrium can be modified significantly, as seen in the ballooning pressure contours of Fig. 7(b). These effects have to be examined more fully, with a self-consistent flow, before deciding on the feasibility of the liquid metal wall concept.

## ACKNOWLEDGEMENT

This work was supported by the U.S. DoE under grant No. DE-FG03-96ER-54346.

## REFERENCES


[1] S. Malang, K. Arheidt, L. Barleon, H. U. Borgstedt, V. Casal, U. Fischer, W. Link, J. Reimann, and K. Rust, Fusion Technology **14**, 1343 (1988).

[2] V. N. Demyanenko, B. G. Karasev, A. F. Kolesnichenko, I. V. Lavrenten, O. A. Lelausis, E. V. Muravev, and A. V. Tananaev, Magnetohydrodynamics **24**, 95 (1988) [Magnitnaya Gidrodinamika **1**, 104 (1988).]

[3] R. W. Moir, Fusion Technology **15**, 674 (1989).

[4] R. D. Woolley, personal communication, 1997. [Presented at the APEX Meeting, UCLA, October 1997.]

[5] L. Zakharov, Bull. Am. Phys. Soc. **7**, 313 (1999).

[6] M. Kotschenreuther, Bull. Am. Phys. Soc. **7**, 214 (1999).

[7] D. Pfirsch and H. Tasso, Nucl. Fusion **11**, 259 (1971).

[8] A. Y. Aydemir and D. C. Barnes, Phys. Rev. Lett. **52**, 930 (1984).

[9] A. Y. Aydemir and D. C. Barnes, J. Comp. Phys. **53**, 100 (1984).

[10] A. Y. Aydemir, Phys. Fluids B **2**, 2135 (1990).

[11] J. Goedbloed, Phys. Fluids **25**, 858 (1982).

[12] H. R. Strauss, D. A. Monticello, and J. Manickam, Nucl. Fusion **29**, 320 (1989).

[13] J. W. Connor, C. G. Gimblett, H. R. Wilson, J. P.Freidberg, and R. J. Hastie, "Stability of resistive wall modes in the presence of walls with poloidally varying rotation", to appear in *Theory of Fusion Plasmas*, Varenna, 2000.

[14] L. Zakharov, Princeton Plasma Physics Laboratory Report No. PPPL-3483 (2000).

[15] E. Hameiri, Phys. Fluids **26**, 230 (1983).